Hindawi
Mathematical Problems in Engineering
Volume 2021, Article ID 3462846, 8 pages
https://doi.org/10.1155/2021/3462846

Research Article

Generation of Digital Art Composition Using a Multilabel Learning Algorithm

Wei Li and Xin Gong

Department of Plastics Arts, Apparel Art Design College, Xi'an polytechnic university, Xi'an 710048, China

Correspondence should be addressed to Wei Li; weili_2021@21cn.com

Received 24 May 2021; Accepted 8 August 2021; Published 9 September 2021

Academic Editor: Hussein Abulkasim

The traditional methods for generating digital art composition have the disadvantage of capturing incomplete geometric information, which leads to obvious defects in the generation results. Therefore, a digital art composition generation method based on the multilabel learning algorithm is proposed in this research. Firstly, a preset series of grids are prepared to generate sampling and fractal pixels on the drawing base. Then, the preset grid construction is constructed by the interactive program of the preset grid library. After the stroke is drawn by the user, the actual motion trajectory of the pen is sampled by the digital panel, and the stroke information in the motion trajectory is obtained by the multilabel learning algorithm. Next, the steps of generating art composition are designed, including generating the skeleton of art composition, generating the geometric network structure of the skeleton, generating the sampling pixel and connecting the fractal pixel, and initializing other attributes of the mesh. Experimental results show that the proposed method has higher sampling rate and geometric information capture rate and has better application performance and prospect.

1. Introduction

As a new form of painting, digital painting is produced and perfected with the continuous development of digital technology [1]. Digital painting inherits the development characteristics of contemporary and modern painting art, including diversification and practicality. Specifically, diversification refers to the diversification of styles and expressions of painting. Before the 20th century, painting styles in each historical period often only had one mainstream form, and one style could represent a specific historical era, such as the Impressionism, Renaissance, and Christianity in the west, as well as scholars, academies, and Taoist schools in China. However, after the 20th century, there were many painting genres at the same time, such as Pop Art, Abstract Expressionism, Surrealism, Expressionism, Abstractionism, Dadaism, Cubism, Fauvism, and other painting genres with different forms of artistic thinking, which emerged one after another and then developed together [2]. In digital painting, these genres are prosperous. Practicality refers to the continuous enhancement of the practicality of the painting and the continuous expansion of the application field. Before the 20th century, whether it is in the east or the west, the expression of the painting was a work of art, and the rich and powerful were keen to regard it as a luxury for collection. In addition to preserving this form, modern painting has also penetrated into various fields. Digital painting has become a basic technical means in many fields, including film, animation, costume design, public art design, architectural landscape design, illustration, and advertising [3]. In the field of digital painting, the problem of digital art composition generation is the current research hotspot [4].

Great attention is paid to the research on the generation of digital art composition. Among them, due to the in-depth research on the digital painting, the international research on the generation of digital art composition has been carried out very early. Some scholars have proposed a digital art composition generation method based on the agent model. The Chinese research on the generation of digital art

composition has only lasted for decades, but certain research results have also been achieved. Some scholars have proposed a digital art composition generation method based on interactive technology.

Because the above methods have problems in sampling and capturing geometric information, a multilabel learning algorithm is applied in the process of research on the digital art composition generation method, and a digital art composition generation method based on multilabel learning algorithm is proposed.

2. Related Works

In this section, related works are reviewed and analyzed.

The objective of Ramanto et al. [5] was to make a framework that could haphazardly produce music that fits the mood from the manual client input. Markov chain is a stochastic model utilized in displaying the segments of the music structure. For the procedurally created to satisfy the mindset of the client, distinctive boundary esteems for every synthesis segment are apportioned for every mindset. These segments incorporate tempo, pitch range, note esteems, harmony type strength, and tune notes. The execution of the procedural music generation framework is then assessed by overviews and analyses. The assessment yielded results that guarantee the capacity of the music generation framework to fit the mood input.

In [6], a modeling technique for advancement is created utilizing an arithmetical model of plan details, prerequisites, and binary codes to apply formal strategies for check, model-based testing, just as techniques for mathematical coordinating. The details of the arithmetical equipment model have conducted polynomial math decided on a bunch of activities and practices.

In [7], a smart music composition neural network is proposed to naturally create a particular style of music. In this construction, the music grouping is obtained through an entertainer's long transient memory and then, at that point, fixed the likelihood of arrangement by a prize-based system that fills in as criticism to improve the exhibition of music synthesis. The music hypothetical principle is acquainted with compelling the style of produced music. A subjective approval in the trial is additionally proposed to ensure the predominance of the model contrasted and cutting edge works.

In [8], first, through the elaboration of the neural network techniques dependent on deep learning, the recurrent neural network (RNN), long short-term memory (LSTM), and gated recurrent unit (GRU) networks were presented, and the deep learning-based GRU-RNN programmed piece model was built. Second, the blockchain innovation was broken down and communicated, and the issues in the conventional copyright security and the board of computerized music were dissected. The three perspectives, i.e., possession, right of utilization, and right insurance, were completely thought of, and the blockchain innovation was incorporated into the copyright security and the board of computerized music. At last, the manual investigation assessment and delay examination were chosen as the pointers to dissect and portray the music structure nature of the GRU-RNN model, just as breaking down the improvement of the computerized music market incorporated with blockchain innovation. The outcomes positively affect advancing the turn of events and the utilization of deep learning strategies and blockchain innovation in computerized music.

It is generally acknowledged that computational advances shape the relationship of performers, instrument manufacturers, and writers with music, influencing different socio-social authenticities in music. In [9], it is reported that the possible ways of music production arise as a social build even because of the common collaboration with human performers and AI-controlled self-ruling instruments. It is contended that structure, making, and performing with a computerized instrument have gone through a slow sociomechanical change that has influenced workmanship, science, innovation, culture, and networks in general.

In [10], a novel technique for creating theoretical artworks is presented. The public artwork dataset WikiArt is utilized, and a K-means calculation is planned that consequently tracks down the ideal K worth to perform shading division on these pictures and partitions the images into various shading blocks. Tests showed that the subsequent unique artistic creation has an extraordinary visual effect, and some of them have been introduced as enhancements openly and private spaces, just as craftsmanship foundations. Likewise, a few specialists and architects have utilized the outcomes in their work.

An algorithm is introduced in [11] to produce digital painting lighting impacts from a solitary picture. The proposed calculation is content-mindful, with created lighting impacts normally adjusting to picture structures, and can be utilized as an intuitive instrument to improve on current labor-intensive work processes for producing lighting impacts for advanced and matte canvases. Likewise, this procedure can deliver usable lighting impacts for photos or three-dimensional delivered pictures. Results show that this methodology can altogether decrease the required collaboration time.

Computer-based intelligence innovation is generally utilized in different fields, including painting. Nonetheless, the mechanical idea of AI painting's own expressive procedures restricts its differentiated determination of painting materials and the setting of brush boundaries, and its showstoppers cannot accomplish the distinctive and acculturated expressive style of the conventional canvas. As a result of science and innovation, with the persistent advancement of science and innovation and the progression of time, the creative substance of works will increment. Advanced innovation ought to be viewed as an apparatus and means for imaginative creation. Just the ideal mix of computerized innovation and conventional composition structures can be helpful for the inventive advancement of workmanship and the feasible improvement of science and innovation and humanities. In light of this, the examination directed in [12] has concentrated on how to rationalistically take a gander at the incorporation of AI innovation and conventional artwork artistic expressions.

According to the discussions that took place, great attention is paid to the research on the generation of digital art composition. Among them, due to the in-depth research on digital painting, international research on the generation of digital art composition has been carried out very early. Generally, some scholars have proposed a digital art composition generation method based on the agent model. In addition, some others have proposed a digital art composition generation method based on interactive technology. However, the current methods have problems in sampling and capturing geometric information. Therefore, in this paper, a new digital art composition generation method based on a multilabel learning algorithm is proposed.

3. Design of the Digital Art Composition Generation Method Based on Multilabel Learning Algorithm

3.1. Preset Grid Construction. In the generation of digital art composition, a series of preset grids must be prepared first to generate sampling primitives and fractal primitives on the painting base [13]. To construct the preset grid through the preset grid library interactive program, the specific operations are as follows:

(1) Initialize the rectangular grid: the user inputs the grid resolution and the rectangular range, and the preset grid library interactive program can generate a uniformly distributed quadrilateral grid in the preset rectangular range and display it to the user [14].

(2) Read a grid in the preset grid library: the user selects a grid from the stored grid library, and the preset grid library interactive program displays the grid to the user [15].

(3) Select the 2D space transformation and apply it to the selected grid: select a transformation in the transformation function library, and enter the default parameters or the parameters that require transformation based on the interface prompts. When inputting the parameters, the user can preview the transformed grid. After the user confirms, the interactive program implements the transformation to the grid [16].

(4) Input the complex variable function to implement the complex transformation of the grid: input the function expression in the form of a string, and the interactive program implements the function to the grid [17]. When applying a complex variable function, the ordinate and abscissa of the grid are calculated as the imaginary and real parts of the complex number.

(5) Save the current grid in the preset grid library.

The specific process of creating the preset grid is shown in Figure 1 [18].

3.2. Get Stroke Information. The tilt, pressure, and position of the digital pen can be sensed by a digital panel. After the user draws the strokes, the digital panel is used to sample the actual motion trajectory of the digital pen, and the stroke information is obtained from the motion trajectory through the multilabel learning algorithm [19].

Five sampling sequences with the same length can be obtained during sampling, as shown in Table 1 [20].

Among the five acquired sampling sequences of the same length, the first four are data acquired by direct sensing digital pens, which need to be preprocessed as follows.

Sequence T is processed into a normalized time within a stroke; that is, the following calculation is performed for the absolute time value [21].

Step 1: conversion to relative time, which is achieved by

$$\begin{cases} t_n = t_n - t_1, \\ t_{n-1} = t_{n-1} - t_1, \\ \dots \\ t_2 = t_2 - t_1, \\ t_1 = 0. \end{cases} \tag{1}$$

Step 2: normalization, which is achieved by

$$t_i = \frac{t_i}{\max\left(t_1, t_2, \dots, t_n\right)}. \tag{2}$$

After the above transformation, $t_1 = 0$, $t_n = 1$, and other parameters are between t_1 and t_n [14].

All the coordinate values of the sequence C are directly transformed from the coordinate values of the drawing board to the coordinate values of the bottom of the drawing [15].

Sequence F is normalized by

$$f_i = \frac{f_i}{\max\left(f_1, f_2, \dots, f_n\right)}. \tag{3}$$

The value in the sequence Θ is directly converted into the corresponding radian value of the included angle of the x-axis [16].

Sequence V is output through these four sequences, and the specific steps are as follows.

Step 1: calculate the absolute speed, which is achieved by

$$\begin{cases} v_{xi} = \dfrac{x_i - x_{i-1}}{t_i - t_{i-1}}, \\ v_{yi} = \dfrac{y_i - y_{i-1}}{t_i - t_{i-1}}, \\ i > 1,\ v_{x1} = v_{x2},\ v_{y1} = v_{y2}. \end{cases} \tag{4}$$

Step 2: normalize the speed, which is achieved by

$$\begin{cases} v_{xi} \longleftarrow \dfrac{v_{xi}}{v_{\max}}, \\ \\ v_{yi} \longleftarrow \dfrac{v_{yi}}{v_{\max}}, \end{cases} \tag{5}$$

where $v_{\max}$ represents the maximum running speed of the digital pen, which is obtained by

$$\begin{cases} v_{\max} & = \max\left(\sqrt{v_{xi}^2 + v_{yi}^2}\right), \\ i & = 1, 2, \ldots, n. \end{cases} \tag{6}$$

The above sequences are all discrete stroke information, which needs to be transformed into a continuous parameter equation [22]. For five sequences, the sequence T is regarded as the parameters of other sequences, and the other sequences are transformed into continuous parameter equations through linear interpolation as expressed by

$$\begin{cases} C(t) = \tau C_i + (1-\tau)C_{i+1}, \\ F(t) = \tau F_i + (1-\tau)F_{i+1}, \\ \Theta(t) = \tau \Theta_i + (1-\tau)\Theta_{i+1}, \\ V(t) = \tau V_i + (1-\tau)V_{i+1}, \end{cases} \quad t \in [t_i, t_{i+1}], \tag{7}$$

where τ represents the continuous parameter threshold, and it can be calculated by

$$\begin{cases} \tau = \dfrac{t - t_i}{t_{i+1} - t_i}, \\ \\ i = 1, 2, \ldots, n. \end{cases} \tag{8}$$

According to the above parameter equations, a multilabel learning algorithm is used to classify and derive the corresponding geometric information of the stroke trajectory [18].

Derived $C(t)$ is expressed in the component form, as given by

$$C(t) = \begin{cases} x(t), \\ y(t), \end{cases} \tag{9}$$

where $x(t)$ and $y(t)$ represent the component coordinates of $C(t)$ [19].

According to the above formula, the corresponding equation of the corresponding tangential parameter $C'(t)$ of the stroke trajectory is given by

$$C'(t) = \begin{cases} x'(t), \\ y'(t), \end{cases} \tag{10}$$

where $x'(t)$ and $y'(t)$ represent the component coordinates of the tangential parameter $C'(t)$ [20].

The equation corresponding to the unit tangential parameter is as follows:

$$C''(t) = \begin{cases} C_x(t) \\ C_y(t) \end{cases} = \begin{cases} \dfrac{x'(t),}{C'(t),} \\ \\ \dfrac{y'(t),}{C'(t),} \end{cases} \tag{11}$$

where $C''(t)$ represents the unit tangential parameter and $C_x(t)$ and $C_y(t)$ represent the component coordinates of the unit tangential parameter.

The normal parameter equation corresponding to the stroke trajectory is as follows:

$$N(t) = \begin{cases} N_x(t) = x'(t)\cos\left(-\dfrac{\pi}{2}\right) - y'(t)\sin\left(-\dfrac{\pi}{2}\right), \\ \\ N_y(t) = x'(t)\sin\left(-\dfrac{\pi}{2}\right) - y'(t)\cos\left(-\dfrac{\pi}{2}\right), \end{cases} \tag{12}$$

where $N(t)$ represents the normal parameter corresponding to the stroke trajectory and $N_x(t)$ and $N_y(t)$ represent the component coordinates of the normal parameter [21].

In this way, one stroke can be used to derive the multiparameter equations of geometric information through the following:

$$\begin{cases} S(t) = \langle C(t), C'(t), C'(t), N(t), N(t), F(t), \Theta(t), V(t) \rangle, \\ t \in [0, 1], \end{cases} \tag{13}$$

where $S(t)$ represents the multiparameter equation group of the derived geometric information, i.e., the stroke information.

3.3. Art Composition Generation. Based on the obtained stroke information, the art composition is generated in four steps. The first step is to generate the skeleton of the art composition, the second step is to generate the geometric network structure of the skeleton, and the third step is to generate sampling primitives and connect fractals. For primitives, the fourth step is to initialize other properties of the grid [23].

The specific steps are as follows:

Step 1: the skeleton of the art composition is the central axis, which is a series of coordinate values obtained by determining the coordinate values of each vertex.

Step 2: extend each node of the skeleton to both sides to generate branch lines with nodes, and connect all branch lines to form a grid. The extension mechanism is controlled by adjusting the preset parameters to control the overall structure of the grid.

Step 3: generate a quadrilateral grid with the same resolution as the fractal primitive; that is, sample the primitive, and connect it with the fractal primitive.

Step 4: the first three steps have determined the specific position of the art composition, and then initialize other parameters based on the preset parameters, including attenuation parameters, image processing functions, activity periods, color channels, and input terminals.

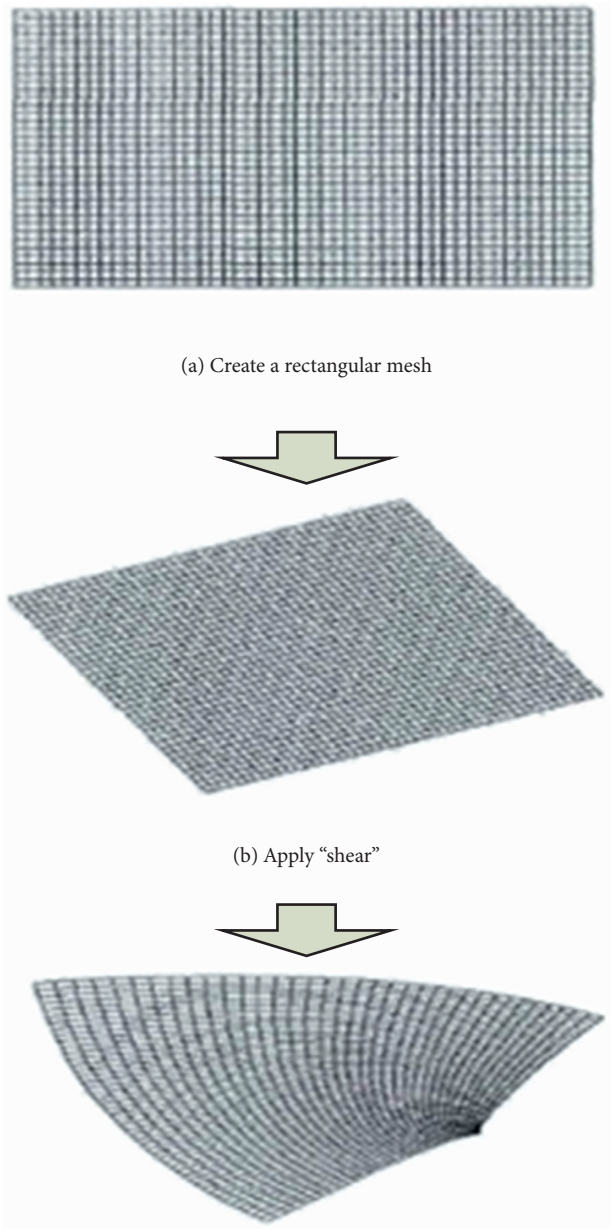

(a) Create a rectangular mesh

(b) Apply "shear"

(c) Imposed transformation "f (z) = Z^2"

Figure 1: The specific process of creating a preset grid.

4. Experiment of Art Composition Generation

4.1. Experimental Design. In order to verify the performance of the digital art composition generation method based on the multilabel learning algorithm, an experiment was carried out. The tool used in the experiment was a digital painting tool, and its framework is shown in Figure 2.

The digital painting tool can implement a total of five painting modes, including collage, prepainting, selection, brush, and color mode. The specific implementation methods are shown in Table 2.

This digital painting tool was used to test the performance of the digital art composition generation method based on multilabel learning algorithm. The sampling rate and geometric information capture rate of this method were obtained and used as experimental data. In order to avoid the lack of convincing results of this experiment, the two existing digital art composition generation methods were used for comparison in the experiment. These two existing digital art composition generation methods included agent-based and interactive technology-based digital art composition generation methods. The performance test of these

Table 1: Five sampling sequences of the same length obtained during sampling.

Sequence marker	Sequence element tags	Meaning
T	$t_1, t_2, \ldots, t_m$	Represents the normalized relative time of each sampling point
C	$C_1 = (x_1, y_1), C_2 = (x_2, y_2), \ldots, C_n = (x_n, y_n)$	Trajectory coordinates of the digital pen on the bottom
F	$f_1, f_2, \ldots, f_n$	Pressure applied to the drawing board by the digital pen
Θ	$\theta_1, \theta_2, \ldots, \theta_n$	Tilt direction of the digital pen
V	$(vx_1, vy_1), (vx_2, vy_2), \ldots, (vx_n, vy_n)$	Indicates the speed of the digital pen during operation

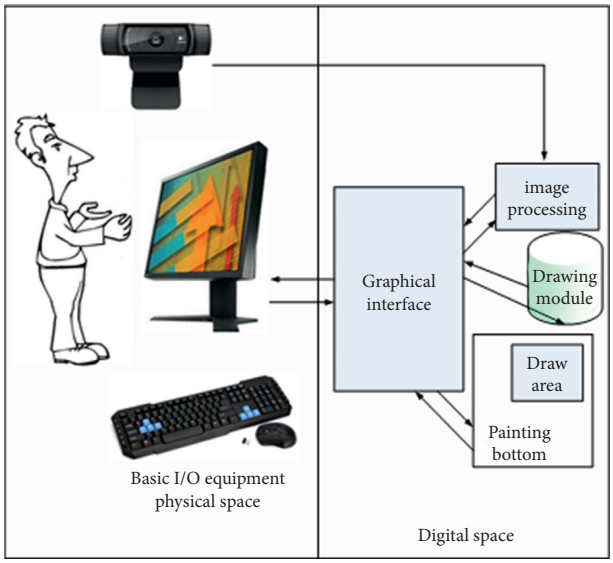

Figure 2: Framework of the digital painting tool.

Table 2: Realization of painting modes.

Number	Painting mode	Implementation mode
1	Color matching mode	Add some color processing methods in image processing, and let users interact through graphics.
2	Brush	The interface specifies the processing parameters and controls the color of the output image.
3	Constituency	An image processing mechanism, which can filter out a special target in the video image.
4	Preprocessing the background	The user can draw with the object in the way of "stroke" in front of the camera.
5	Collage	Let the user specify a specific area on the bottom of the painting. When painting, the pigment can only affect the selected area.

two methods was also performed, and the sampling rate and geometric information capture rate of these two methods were obtained and used as comparative experimental data. The sampling rate and geometric information capture rate of the three digital art composition generation methods are analyzed and compared.

4.2. Experimental Results

4.2.1. Sampling Rate. In the test of digital art composition generation, the sampling rate data of the digital art composition generation method based on the multilabel learning algorithm and based on the agent model and interactive technology are shown in Table 3. In addition, the results are also displayed in Figure 3 for a better comparison.

According to Table 3 as well as Figure 3, in the test of digital art composition generation, the sampling rate of the digital art composition generation method based on the multilabel learning algorithm was higher than that of the method based on the agent model and interactive technology.

4.2.2. Geometric Information Capture Rate. Table 4 presents the geometric information capture rate of the digital art composition generation method based on the multilabel learning algorithm, agent model, and interactive technology. In addition, the results are also displayed in Figure 4 for a better comparison.

According to Table 4 as well as Figure 4, in the test of digital art composition generation, the geometric information capture rate of the digital art composition generation method based on the multilabel learning algorithm was higher than that of the method based on the agent model and interactive technology.

Based on the above experimental results, the sampling rate and geometric information capture rate of the digital art

Table 3: Experimental data of sampling rate.

Grid size	Sampling rate (frame/s)		
	Method based on multilabel learning algorithm	Method based on the agent model	Method based on interactive technology
1 × 1	32.5	25.3	22.3
2 × 2	30.8	23.6	20.4
3 × 3	28.6	22.9	17.3
4 × 4	26.7	21.3	16.8
5 × 5	25.1	21.0	15.2
6 × 6	23.8	18.0	13.7
7 × 7	21.7	15.9	11.7
8 × 8	18.2	15.2	10.2
9 × 9	17.9	13.2	9.3
10 × 10	17.2	11.8	9.0

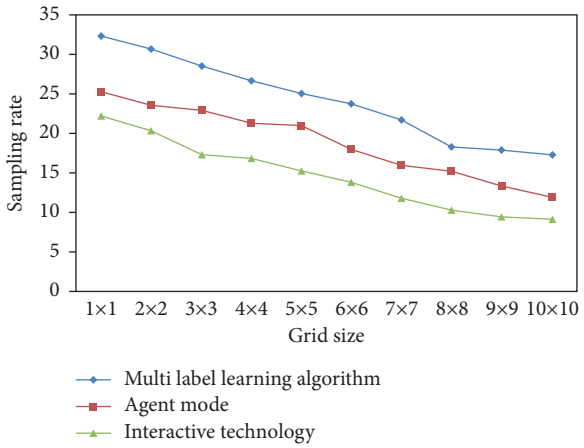

Figure 3: Results of the sampling rate.

Table 4: Experimental data of geometric information capture rate.

Grid size	Geometric information capture rate (%)		
	Method based on multilabel learning algorithm	Method based on the agent model	Method based on interactive technology
1 × 1	98.34	94.23	89.62
2 × 2	98.32	94.22	89.60
3 × 3	98.30	94.19	89.59
4 × 4	98.27	94.17	89.61
5 × 5	98.25	94.15	89.58
6 × 6	98.21	94.13	89.50
7 × 7	98.20	94.11	89.54
8 × 8	98.18	94.18	89.53
9 × 9	98.17	94.08	89.50
10 × 10	98.13	94.10	89.55

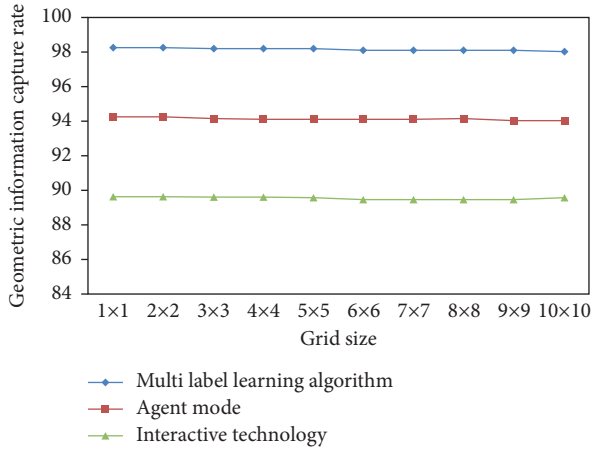

Figure 4: Results of the geometric information capture rate.

composition generation method based on the multilabel learning algorithm were higher than those of the two comparative digital art composition generation methods, indicating its better performance.

5. Conclusion

By designing a digital art composition generation method based on multilabel learning algorithm, the sampling rate and geometric information capture rate are improved. However, the stroke information data obtained in the design of the method contain redundant data, and the processing of the redundant data will be investigated in the future.

Data Availability

All the data used to support the findings of this study are available from the corresponding author upon reasonable request.

Conflicts of Interest

The authors declare that there are no conflicts of interest.

References

[1] B. Coşkun Onan, "Implementing contemporary art theory to instruction of painting in undergraduate level: a phenomenology study," *Uludağ Üniversitesi Eğitim Fakültesi Dergisi*, vol. 30, no. 2, pp. 725–755, 2018.

[2] C. Schmidt, M. Santos, L. Bohn et al., "Dynamic balance and mobility explain quality of life in HFpEF, outperforming all the other physical fitness components," *Arquivos Brasileiros de Cardiologia*, vol. 114, no. 4, pp. 701–707, 2020.

[3] D. Aras, C. Ç. Bildircin, Ö. Güler, M. Gülü, and F. Akça, "Spor tirmaniş yetenek Seçimi test bataryasi Örneği," *Ankara Üniversitesi Beden Eğitimi ve Spor Yüksekokulu SPORMETRE Beden Eğitimi ve Spor Bilimleri Dergisi*, vol. 17, no. 2, pp. 41–52, 2019.

[4] F. Schwalbe, "The importance of student leagues on medical training in neurosurgery and residency choice," *Arquivos Brasileiros De Neurocirurgia Brazilian Neurosurgery*, vol. 37, no. 01, pp. 13–18, 2018.

[5] R. Ramanto, A. Sigit, and N. U. Maulidevi in *Proceedings of the ADADA 2016 14TH international Conference for Asia Digital Art and Design Association-Mood-based Procedural Music Generation Using Markov Chains*, Bali, Indonesia, November 2016.

[6] O. O. Letychevskyi, V. S. Peschanenko, V. S. Kharchenko, V. A. Volkov, and O. M. Odarushchenko, "Modeling method for development of digital system Algorithms based on programmable logic devices," *Cybernetics and Systems Analysis*, vol. 56, no. 5, pp. 710–717, 2020.

[7] C. Jin, Y. Tie, Y. Bai, X. Lv, and S. Liu, "A style-specific music composition neural network," *Neural Processing Letters*, vol. 52, no. 3, pp. 1893–1912, 2020.

[8] H. Li, "Piano automatic computer composition by deep learning and blockchain technology," *IEEE Access*, vol. 8, pp. 188951–188958, 2020.

[9] K. Tahiroğlu, "Ever-shifting roles in building, composing and performing with digital musical instruments," *Journal of New Music Research*, vol. 50, no. 2, pp. 155–164, 2021.

[10] M. Li, J. Lv, J. Wang, and Y. Sang, "An abstract painting generation method based on deep generative model," *Neural Processing Letters*, vol. 52, pp. 1–12, 2019.

[11] L. Zhang, E. Simo-Serra, Ji Yi, and C. Liu, "Generating digital painting lighting effects via RGB-space geometry," *ACM Transactions on Graphics*, vol. 39, no. 2, pp. 1–13, 2020.

[12] X. Liu, "Artistic reflection on artificial intelligence digital painting," in *Journal of Physics: Conference Series*vol. 1648, no. 3, IOP Publishing, Article ID 032125, 2020.

[13] H. Liu, Z. Mi, L. Lin et al., "Shifting plant species composition in response to climate change stabilizes grassland primary production," *Proceedings of the National Academy of Sciences*, vol. 115, no. 16, pp. 4051–4056, 2018.

[14] G. Incerti, E. Cecconi, F. Capozzi et al., "Infraspecific variability in baseline element composition of the epiphytic lichen Pseudevernia furfuracea in remote areas: implications for biomonitoring of air pollution," *Environmental Science and Pollution Research*, vol. 24, no. 9, pp. 1–13, 2020.

[15] X. Gan, G. Xu, G. Zhao, M. Zhou, and Z. Cai, "Composition optimization of Nb-Ti microalloyed high strength steel," *Journal of Wuhan University of Technology-Mater. Sci. Ed.*, vol. 33, no. 5, pp. 1193–1197, 2018.

[16] J. Liu, S. Du, F. Li, H. Zhang, and S. Zhang, "Preparation of ZrB2-SiC powders via carbothermal reduction of zircon and prediction of product composition by back-propagation artificial neural network," *Journal of Wuhan University of Technology-Mater. Science Education*, vol. 33, no. 5, pp. 1062–1069, 2018.

[17] Z. Dongdong, G. Hao, L. Jingfeng et al., "Effect of Cu-Ti-C reaction composition on reinforcing particles size of TiC x/Cu composites," *Journal of Wuhan University of Technology-Mater. Science Education*, vol. 33, no. 1, pp. 43–48, 2018.

[18] E. S. M. Younis, A. S. Al-Quffail, N. A. Al-Asgah et al., "Effect of dietary fish meal replacement by red algae, Gracilaria arcuata, on growth performance and body composition of Nile tilapia *Oreochromis niloticus*," *Saudi Journal of Biological Sciences*, vol. 25, no. 2, pp. 198–203, 2017.

[19] B. O. Otegbayo, D. J. Oguniyan, B. A. Olunlade, O. O. Oroniran, and O. E. Atobatele, "Characterizing genotypic variation in biochemical composition, anti-nutritional and mineral bioavailability of some Nigerian yam (Dioscorea spp.) land races," *Journal of Food Science and Technology*, vol. 55, no. 1, pp. 205–216, 2018.

[20] B. Basu, O. Chowdhury, and S. Saha, "Possible link between stress-related factors and altered body composition in women with polycystic ovarian syndrome," *Journal of Human Reproductive Sciences*, vol. 11, no. 1, pp. 10–18, 2018.

[21] J. Leskovec, A. Levart, S. A. Nemec et al., "Effects of supplementation with α-tocopherol, ascorbic acid, selenium, or their combination in linseed oil-enriched diets on the oxidative status in broilers," *Poultry Science*, vol. 97, no. 1, pp. 86–93, 2018.

[22] M. Alessandra, D. Z. Antonio, E. Graziana et al., "Age-related changes to human tear composition," *Investigative Ophthalmology & Visual Science*, vol. 59, no. 5, pp. 2024–2031, 2018.

[23] N. Royaei, T. Shahrabi, and Y. Yaghoubinezhad, "The investigation of the electrocatalytic and corrosion behavior of a TiO2-RuO2 anode modified by graphene oxide and reduced graphene oxide nanosheets via a sol-gel method," *Catalysis Science & Technology*, vol. 8, no. 19, pp. 4957–4974, 2018.